

Cell expansion of human articular chondrocytes on macroporous gelatine scaffolds: — impact of micro carrier selection on cell proliferation

Sofia Pettersson, Jonas Wetterö, Pentti Tengvall and Gunnar Kratz

Linköping University Post Print

N.B.: When citing this work, cite the original article.

Original Publication:

Sofia Pettersson, Jonas Wetterö, Pentti Tengvall and Gunnar Kratz, Cell expansion of human articular chondrocytes on macroporous gelatine scaffolds: — impact of micro carrier selection on cell proliferation, 2011, Biomedical Materials, (6), 6, 065001.

<http://dx.doi.org/10.1088/1748-6041/6/6/065001>

Copyright: Institute of Physics

<http://www.iop.org/>

Postprint available at: Linköping University Electronic Press

<http://urn.kb.se/resolve?urn=urn:nbn:se:liu:diva-54114>

Cell expansion of human articular chondrocytes on macroporous gelatine scaffolds – impact of microcarrier selection on cell proliferation

Sofia Pettersson^{1,5}, Jonas Wetterö², Pentti Tengvall³ and Gunnar Kratz^{1,4}

¹ Laboratory for Reconstructive Plastic Surgery, Dept. of Clinical and Experimental Medicine, Linköping University, SE-581 85 Linköping, Sweden

² Rheumatology/AIR, Dept. of Clinical and Experimental Medicine, Linköping University, SE-581 85 Linköping, Sweden

³ Institute of Clinical Sciences, Dept. of Biomaterials, The Sahlgrenska Academy at University of Gothenburg, Gothenburg, Sweden

⁴ Dept. of Hand, Plastic, and Burn Surgery, University Hospital of Linköping, SE-581 85 Linköping, Sweden

Experimental work performed at the Laboratory for Reconstructive Plastic Surgery, Dept. of Clinical and Experimental Medicine, Linköping University, Linköping, Sweden

Address for correspondence:

⁵ Div. of Information Coding, Dept. of Electrical Engineering, Linköping University, SE-581 83 Linköping, Sweden

E-mail: sofia.pettersson@liu.se

Abstract

This study investigates human chondrocyte expansion on four macroporous gelatine microcarriers (CultiSpher) differing with respect to two manufacturing processes – the amount of emulsifier used during initial preparation and the gelatine cross-linking medium. Monolayer-expanded articular chondrocytes from three donors were seeded onto the microcarriers and cultured in spinner flask systems for a total of 15 days. Samples were extracted every other day to monitor cell viability and establish cell counts, which were analyzed using analysis of variance (ANOVA) and piecewise linear regression. Chondrocyte densities increased according to a linear pattern for all microcarriers, indicating an ongoing, though limited, cell proliferation. A strong chondrocyte donor effect was seen during the initial expansion phase. The final cell yield differed significantly between the microcarriers and our results indicate that manufacturing differences affected chondrocyte densities at this point. Remaining cells stained positive for chondrogenic markers SOX-9 and S-100 but extracellular matrix formation was modest to undetectable. In conclusion, the four gelatine microcarriers supported chondrocyte adhesion and proliferation over a two-week period. The best yield was observed for microcarriers produced with low emulsifier content and cross-linked in water and acetone. These results add to the identification of optimal biomaterial parameters for specific cellular processes and populations.

PACS

- 87.85.Lf Tissue Engineering
- 87.85.J Biomaterials
- 87.17.Ee Growth and division
- 87.14.E Proteins

Submitted to *Biomedical Materials*.

1. Introduction

The need for fast, reliable and economic cell expansion is a priority issue for tissue engineering of cartilage. Vast numbers of cells are frequently needed, as the initial cell density can have a dramatic influence on the final outcome (Mauck *et al.*, 2003; Eyrich *et al.*, 2007). Conventional cell expansion techniques, such as monolayer cell culture, can cause chondrocytes to dedifferentiate into a fibroblast-like cell type, making the balance between cell expansion and phenotype integrity a delicate issue (Holtzer *et al.*, 1960; von der Mark *et al.*, 1977). One approach that enables chondrocyte expansion and improves redifferentiation potential is microcarrier-based cell culture (Fronzoza *et al.*, 1996; Malda *et al.*, 2003a; Malda *et al.*, 2003b). Microcarrier-based cell culture was first developed as a means to increase the surface area for anchorage-dependent cells, but has since developed into a unique field with a wide variety of microcarriers for cell culture and tissue engineering available (van Wezel, 1967; Kong *et al.*, 1999; Malda and Fronzoza, 2006). The choice of microcarrier can have significant effects on the outcome as biomaterial porosity, surface chemistry and surface topography can affect cell adhesion, morphology, phenotype and proliferation (Boyan *et al.*, 1996; Chung *et al.*, 2008; Costa Martinez *et al.*, 2008; Curtis and Wilkinson, 1997; Kong *et al.*, 1999; Lee *et al.*, 1994; Wu *et al.*, 2008). A porous structure enhances the available culture surface area further and interconnected pores enable cell migration as well as cell–cell signalling throughout the scaffold (Chung *et al.*, 2008; Nilsson, 1988).

Macroporous Cultispher gelatine microcarriers support cell adhesion and growth of several human and animal cell types (Fernandes *et al.*, 2007; Huss *et al.*, 2007; Liu *et al.*, 2004; Malda *et al.*, 2003a; Melero-Martin *et al.*, 2006; Ohlson *et al.*, 1994; Werner *et al.*, 2000). Previous findings have shown that scale-up of chondroprogenitor cells can be achieved by adding empty microcarriers and gradually increasing the culture volume in the spinner flasks (Melero-Martin *et al.*, 2006). This bead-to-bead transfer had previously been reported for Chinese hamster ovary cells with the same type of microcarrier (Ohlson *et al.*, 1994). Furthermore, in a recent study, investigators have cryo-preserved cell-seeded microcarriers (Lippens and Cornelissen, 2010). Combined, these features enable cells to be expanded, preserved, transported and transplanted in an anchored state without exposure to trypsin, making this type of microcarrier suitable as biodegradable scaffolds for tissue regeneration. We have previously proposed the use of gelatine microcarriers in combination with platelet rich plasma as a delivery system for tissue engineering of cartilage using both human dermal fibroblasts, subjected to chondrogenic induction media, and human articular chondrocytes (Sommar *et al.*, 2009; Pettersson *et al.*, 2009). Other investigators have also used this type of microcarrier in combination with human chondrocytes (Malda *et al.*, 2003a; Pettersson *et al.*, 2009; Huss *et al.*, 2007; Schrobback *et al.*, 2011). There is however limited knowledge regarding the optimal choice of microcarrier for chondrocyte expansion.

This study is focused on studying the role of microcarrier selection for chondrocyte expansion. The four microcarrier variants investigated vary with respect to two manufacturing procedures – the

amount of emulsifier used during the initial stages of preparation and the chemical environment in which gelatine cross-linking takes place (Nilsson, 2008). The amount of emulsifier can be adjusted as a means to control the average pore size of the macroporous structures. For the currently investigated microcarriers a nonionic emulsifier and surfactant, Tween 80, is used during production (Nilsson, 2008). By increasing the amount of surfactant during the initial steps, the resulting microcarriers (GL- and GLS-type) obtain a larger average pore size compared to the microcarriers produced with a relatively lower emulsifier concentration (G- and S-type). The gelatine in these microcarriers is subsequently cross-linked using hexamethylene diisocyanate, a non-zero length cross-linking agent that breaks down rapidly in water, forming hexamethylene diamine. Cross-linking is accomplished through the reaction of free amine groups of lysine and hydroxylysine, or free carboxylic acid residues of glutamic and aspartic acid of the protein molecule (Kuijpers *et al.*, 2000). For the two types of cross-linking described here, the cross-linking procedure involves the addition of hexamethylene diisocyanate and triethylamine to the gelatine mixed either in water alone (S-type) or in a mixture of water and acetone (G-type) (Nilsson, 2008). The former method results in microcarriers with a higher thermal and mechanical stability, that releases less material into the cell culture medium than the G-type counterparts (Kong *et al.*, 1999).

The aim of this study is to evaluate cell expansion of human articular chondrocytes on four different macroporous gelatine microcarriers and investigate possible influences on the final cell yield.

2. Materials and methods

Unless otherwise indicated, all chemicals were obtained from Gibco-Invitrogen (Carlsbad, CA). All cell cultures were maintained at 37°C, 5.0% CO₂ and 95% humidity.

2.1. Microcarriers

Macroporous CultiSpher gelatine microcarriers were kindly supplied by Percell Biolytica AB (Åstorp, Sweden) and prepared according to the manufacturer's recommendations. Four different variants were used – CultiSpher G (CS-G), CultiSpher S (CS-S), CultiSpher GL (CS-GL) and CultiSpher GLS (CS-GLS). General specifications of these microcarriers, as specified by the manufacturer, are listed in table 1. In short, 0.1 g (dry weight) of microcarriers were rehydrated in 5 mL Ca²⁺- and Mg²⁺-free phosphate buffered saline (PBS) (pH 7.4, Medicago AB, Uppsala, Sweden) for a minimum of one hour and sterilized by autoclaving (121°C, 20 min, 80°C cooling temperature, 2.8 bar). Sterilized microcarriers were washed in PBS and cell culture medium, and stored at 4°C in cell culture medium until further use. Each type of microcarrier was prewarmed to 37°C in individual 250 mL spinner flasks (Techne, Staffordshire, U.K.) prior to cell seeding.

Table 1. General specifications for the microcarriers.

CultiSpher	G	S	GL	GLS
Cross-linking environment ^a	H ₂ O + C ₃ H ₆ O	H ₂ O	H ₂ O + C ₃ H ₆ O	H ₂ O
Emulsifier amount ^b	Low	Low	High	High
Particle diameter (μm) ^c	130-380	130-380	166-370	100-200
Average pore diameter (μm) ^c	20	20	30	30
Volume (mL/g dry) ^c	12-18	10-16	12	12
Density (g/mL) ^c	1.04	1.04	1.04	1.04
Number per unit weight ^d	1000000	800000	1000000	1000000

^a Medium in which cross-linking of the microcarriers takes place during manufacturing.

^b Relative amount during first emulsion step during manufacturing.

^c Rehydrated in PBS.

^d Microcarriers/g dry.

2.2. Microcarrier characterization

Scanning electron microscopy (SEM) and light microscopy were used to study microcarrier features. For SEM, dehydrated microcarriers were attached to a stub and sputtered with a 15-μm layer of platinum prior to microscopy. SEM images were retrieved at a 45° angle with a JSM-840 microscope (Jeol Ltd., Tokyo, Japan). For light microscopy, hydrated, sterilized and washed microcarriers were placed under a cover slip and immediately examined with a BX41 microscope (Olympus Optical Co., Tokyo, Japan).

2.3. Cell culture

The cell culture medium used for all chondrocyte cell culture, was Dulbecco's Modified Eagle's Medium (DMEM), supplemented with 10% heat inactivated (45 min at 57°C) newborn calf serum (NCS), 10 mM HEPES (Sigma-Aldrich Chemie GmbH, Steinheim, Germany), 0.1 mM MEM non-essential amino acids, 0.4 mM L-proline (Sigma-Aldrich), 50 g/mL L-ascorbic acid (Sigma-Aldrich), 50 U/mL penicillin and 50 μg/mL streptomycin. Human articular chondrocytes were isolated from three different donors (table 2) following total knee arthroplasties, without specific knowledge of donor identities according to national ethical regulations. The tissue was dissected into 1–3 mm³ pieces and the cartilage enzymatically digested overnight in a mixture of collagenase type II (350 U/mL) and dispase (2.5 U/mL) in DMEM with 2% fetal calf serum (FCS). The isolated cells were washed in cell culture medium and plated in 75 cm² polystyrene cell culture flasks (BD Biosciences, Franklin Lakes, NJ). Medium was changed 2–3 times per week and cells grown at 37°C, 5.0% CO₂ and 95% humidity. Cells were passaged by washing flasks with 0.02% ethylene diamine tetra-acetic acid (EDTA, ICN Biomedicals, Aurora, OH) prior to enzymatic detachment in 0.01% EDTA/0.125% trypsin at 37° C for approximately 15–20 min. When cryopreserved, cells were detached as described above, washed and resuspended in 80% FCS with 10% DMEM and 10% DMSO (Sigma-Aldrich). Cells were frozen at -70°C and transferred to liquid nitrogen tanks. Once thawed, cells were immediately washed in cell culture medium before plating in polystyrene culture flasks.

Table 2. Articular chondrocytes were isolated from the following three donors.

Donor	Sex	Age	Passage ^a	Cell count ^b	Viable cell count ^b
1	F	67	P2	7.5×10^6	7.1×10^6
2	M	37	P3	7.5×10^6	7.4×10^6
3	M	56	P3	7.5×10^6	7.2×10^6

^a Passage number at microcarrier seeding.

^b Total and viable cell count that were seeded per 0.1 g dry weight microcarrier.

2.4. Cell counting

Cell counts were established using a Guava PCA cytometer and the CytoSoft 2.1 ViaCount Assay software application (Guava Technologies, Hayward, CA). According to the manufacturer's recommendation, all samples were stained with Guava ViaCount Reagent for a minimum of 5 min, to allow the fluorescent dyes to bind to the cells. Cell solutions were thoroughly mixed prior to dilutions and assays. Information on the number of dilutions per sample, dilution factors and number of events acquired for each application can be found below.

2.5. Cell seeding on microcarriers

Chondrocytes were detached as described above, washed to remove trypsin residues, and resuspended in cell culture medium. Triplicate samples were removed for cell counting, where double dilutions (1:20) were prepared for each sample and 1000 events acquired for each dilution. The original cell suspension was thoroughly mixed and a total of 7.5×10^6 cells per 0.1 g microcarrier (dry weight) was added to each spinner flask with a 50 mL working volume of cell culture medium. The initial cell-seeding density was chosen within the recommended cell-seeding range ($5\text{--}20 \times 10^7$ cells per gram dry weight according to the manufacturer). Stirring was set to intermittent stirring (Techne MCS-104S, 5 min at 30 rpm, 55 min rest) for the initial 24-hour period, after which time the medium volume was adjusted to 100 mL and stirring set to continuous mode (30 rpm). Chondrocyte passage number and viable cell count at microcarrier seeding for the different donors can be found in table 2.

2.6. Microcarrier sampling and cell counting

Microcarriers were allowed to settle for 15 min before 50 mL medium was removed and discarded from each spinner flask. A total of five 0.5 mL samples of well-distributed microcarrier solution were drawn from each flask. In addition, a 0.4 mL sample was taken from each flask for viability assay (see below). After sampling, fresh cell culture medium (50 mL) was added to the culture flasks and flasks returned to the incubator. After sedimentation of the sample microcarriers, the supernatant was discarded and the microcarriers were incubated with trypsin (0.125%)/EDTA (0.01%). Samples were left in room temperature, with occasional micropipette mixing, for approximately 20–40 min until the microcarriers had dissolved. Each sample was diluted (1:5) and counted once (500–1000 events acquired, or until instrument time out after 2 min).

Microcarrier impact on chondrocyte expansion

2.7. *MTT viability assay*

Cell viability on the gelatine microcarriers was visualized with a 3-(4, 5-dimethylthiazol-2-yl)-2, 5-diphenyltetrazolium bromide (MTT) assay. For each group, a 0.4 mL sample of evenly distributed microcarrier suspension was incubated with 0.5 mg/mL MTT (Sigma-Aldrich) for 45 min at 37°C. Staining was evaluated immediately using an IX51 inverted light microscope and images retrieved with a DP70 CCD camera and DP Controller software (version 1.1.1.65, Olympus Optical Co., Tokyo, Japan).

2.8. *Histological and immunohistochemical staining*

After the last sampling, remaining microcarriers (n=2 donors) were collected from the spinner flasks, washed in PBS and fixed in 4% neutral buffered formaldehyde for approximately 12 hours. The washed and dehydrated microcarriers were embedded in Histowax (Histolab products AB, Göteborg, Sweden) after which six- μ m thick sections were generated with a microtome (Leica Microsystems GmbH, Wetzlar, Germany), and mounted on Superfrost Plus slides (Menzel GmbH, Braunschweig, Germany). All sections were deparaffinized and rehydrated in an ethanol series prior to staining. For histology, sections were incubated in 1% Alcian Blue (w/v in 0.1 M HCl) for 30 min at room temperature, rinsed with water and acetic acid (0.1%) and counterstained with nuclear red for 5 min. For indirect immunohistochemistry, sections were treated with 0.25% ammonia (NH₃) in 70% ethanol for 1 hour during dehydration (Baschong *et al.*, 2001), and incubated 1 hour in 0.1 M glycine in PBS to quench autofluorescence. For SOX-9 and S-100, heat mediated antigen retrieval in 10 mM Tris/1 mM EDTA buffer (pH 9) was performed at 95°C for 20 min. Non-specific binding was blocked with 5% bovine serum albumin (BSA, Sigma) for 1 hour prior to incubation with rabbit polyclonal antibody against SOX-9 (1:100, Abcam plc, Cambridge, UK) or rabbit antibody against S-100 (1:400, Dako A/S, Glostrup, Denmark) overnight at 4°C. For aggrecan, antigen retrieval was performed with 0.1 U/mL Chondroitinase ABC (Sigma-Aldrich) in 50 mM Tris-HCl buffer containing 60 mM sodium acetate (Merck) at pH 8 for 45 min at 37°C. Non-specific binding was blocked with 5% BSA prior to incubation with a mouse monoclonal anti-aggrecan antibody diluted in PBS (clone 6-B-4, 1:50, Abcam) overnight at 4°C. Negative controls were incubated in PBS only. Sections were washed rigorously and subsequently incubated with the corresponding Alexa Fluor 488 antibody (1:500, Molecular Probes, Invitrogen) for one hour at room temperature, and mounted with ProLong Gold antifade reagent containing DAPI (Molecular Probes). Sections were examined with an Olympus BX41 microscope, using ultraviolet, blue and green filters (MWU2, MWIB2 and MWIG2, Olympus). A high-resolution digital Olympus DP70 CCD camera was used to acquire images.

Microcarrier impact on chondrocyte expansion

2.9. Image processing

All image adjustments were made for the sole purpose of enhancing printing clarity, using Photoshop CS3 (Adobe Systems Inc., San Jose, CA). For montages of stained sections, identical adjustments were made for all equivalent images.

2.10. Data processing and statistical analysis

For graphs, the cell count \times (cells/mL) was normalized to cell density per 0.1 g (dry weight) gelatine microcarrier, the original amount of microcarriers in the spinner flask. The graphs in figures 3 and 4a, including means, standard errors and standard deviations, were prepared with GraphPad Prism (v5.0a, GraphPad Software Inc., La Jolla, CA). Analysis of variance (ANOVA) was performed using all cell count data to compare microcarrier groups at each time point with one fixed factor (microcarrier) and one random factor (donor). Piecewise linear regression was performed using all cell count data with a break point at day 7 and ANOVA of the regression line slopes and levels was performed with one fixed factor (microcarrier) and one random factor (donor) to analyze differences between the microcarriers, or with two fixed factors (cross-linking environment and emulsifier concentration) and one random factor (donor) to analyze differences with regards to the microcarrier properties. Differences in the slopes of regression lines before and after the break point were analyzed. Differences in the levels of regression lines were analyzed in the middle of each interval (day 4 and day 12 respectively) as well as at the end of the culture period (day 15). Tukey simultaneous tests for pairwise comparisons were conducted when significant differences were found. ANOVA, piecewise linear regression and Tukey analysis were performed using Minitab (Minitab Inc., State College, PA).

3. Results

3.1. Microcarrier structure

SEM revealed differences in microcarrier macrostructure between the four groups (figure 1a). The data from table 1 allows for differences in microcarrier diameters, yet the CS-GLS microcarrier directly distinguished itself with a non-spherical form (figure 1a, bottom right). In general, CS-S and CS-GLS microcarriers displayed less spherically shaped and more elongated pores (figure 1a, right column), compared to CS-G and CS-GL (figure 1a, left column). We found differences in pore diameters and overall porosity on individual microcarrier surfaces, where certain regions contained more or less closed-off pores. This was observed in all microcarrier groups (data not shown). A closer look at the matrices revealed presence of wrinkles, micropores (with diameters $<10 \mu\text{m}$) and craters on the surfaces of all microcarrier types (figure 1b). After rehydration and sterilization the gelatine matrices swell (figure 1c). The porous features of the hydrated microcarriers were more difficult to discern with light microscopy, yet pores in the reported range are visible, with CS-GL and CS-GLS (figure 1c, bottom row) displaying larger pore diameters than their CS-G and CS-S

Microcarrier impact on chondrocyte expansion

counterparts (figure 1c, top row). Several heterogeneously sized pores were visible in the gelatine at higher magnification images (figure 1d).

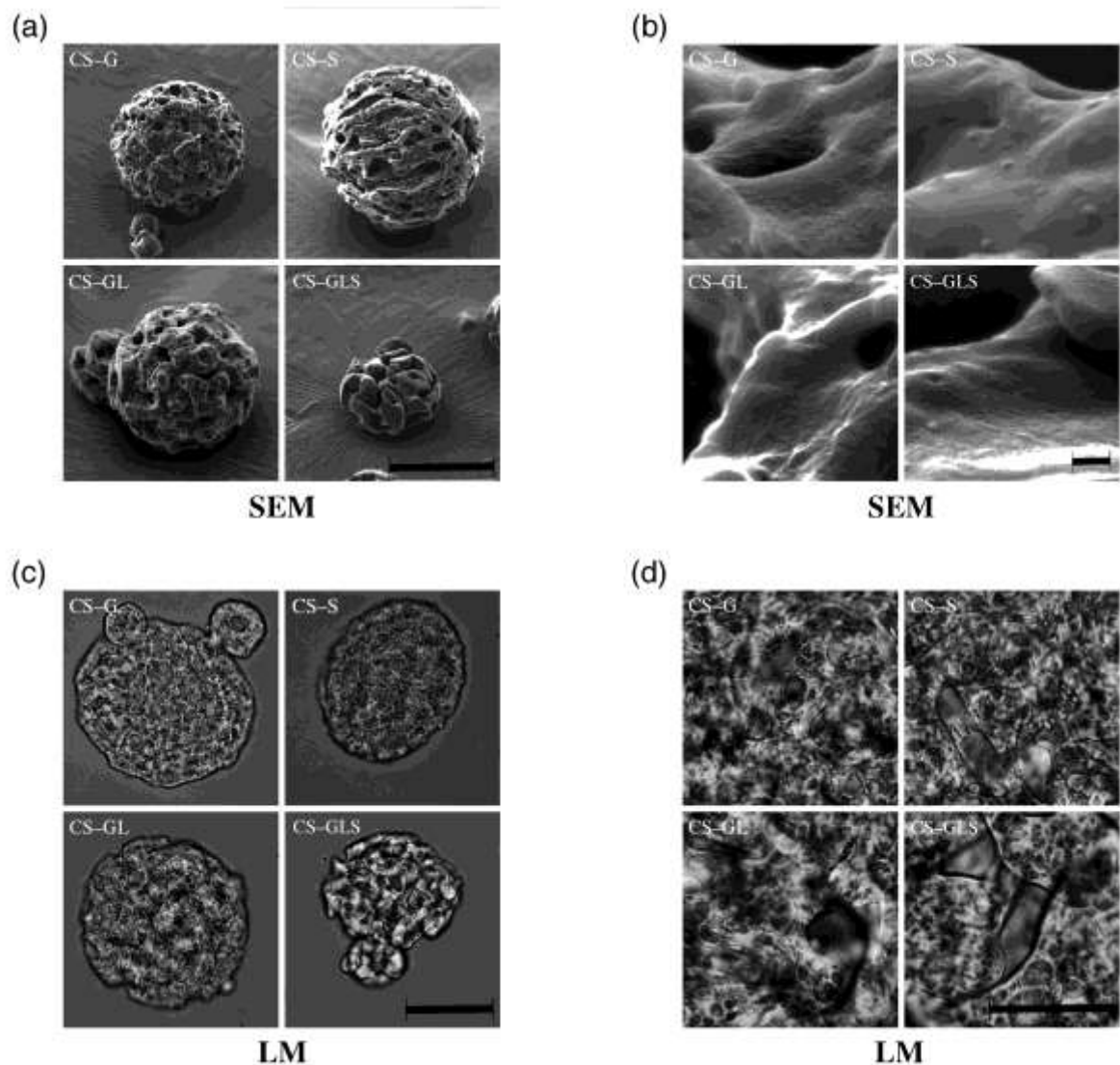


Figure 1. Scanning electron microscopy (SEM) of dehydrated microcarriers (a-b). Light microscopy (LM) of rehydrated, sterilized and washed microcarriers (c-d). Scale bars 100 μm (a), 1 μm (b), 125 μm (c) and 50 μm (d) respectively.

3.2. Viability and sampling

Viable cells, as indicated by the MTT viability assay, were found on all four microcarrier types at each sampling (full data not shown). After 24 hours viable cells could be found in all groups, but not on each individual microcarrier (figure 2a). An increased amount of viable chondrocytes was found after 5 days and by this time microcarrier aggregates had begun to form (figure 2b). As chondrocyte density increased further, several large aggregates with cell-cell interactions forming cellular bridges between the microcarriers were found for all microcarrier groups (figure 2c-d). At the final time point individual chondrocytes were hard to distinguish due to a high chondrocyte density (figure 2d). Light

Microcarrier impact on chondrocyte expansion

to medium pipetting was needed to ensure homogenous microcarrier dispersions in the spinner flasks prior to sampling. The amount of time required to fully dissolve the microcarriers approached or exceeded 30 min, and increased with the microcarrier cell densities. For the acquired samples, vigorous micro-pipetting was required to ensure a homogenous cell solution for cell count procedures once the microcarriers were dissolved.

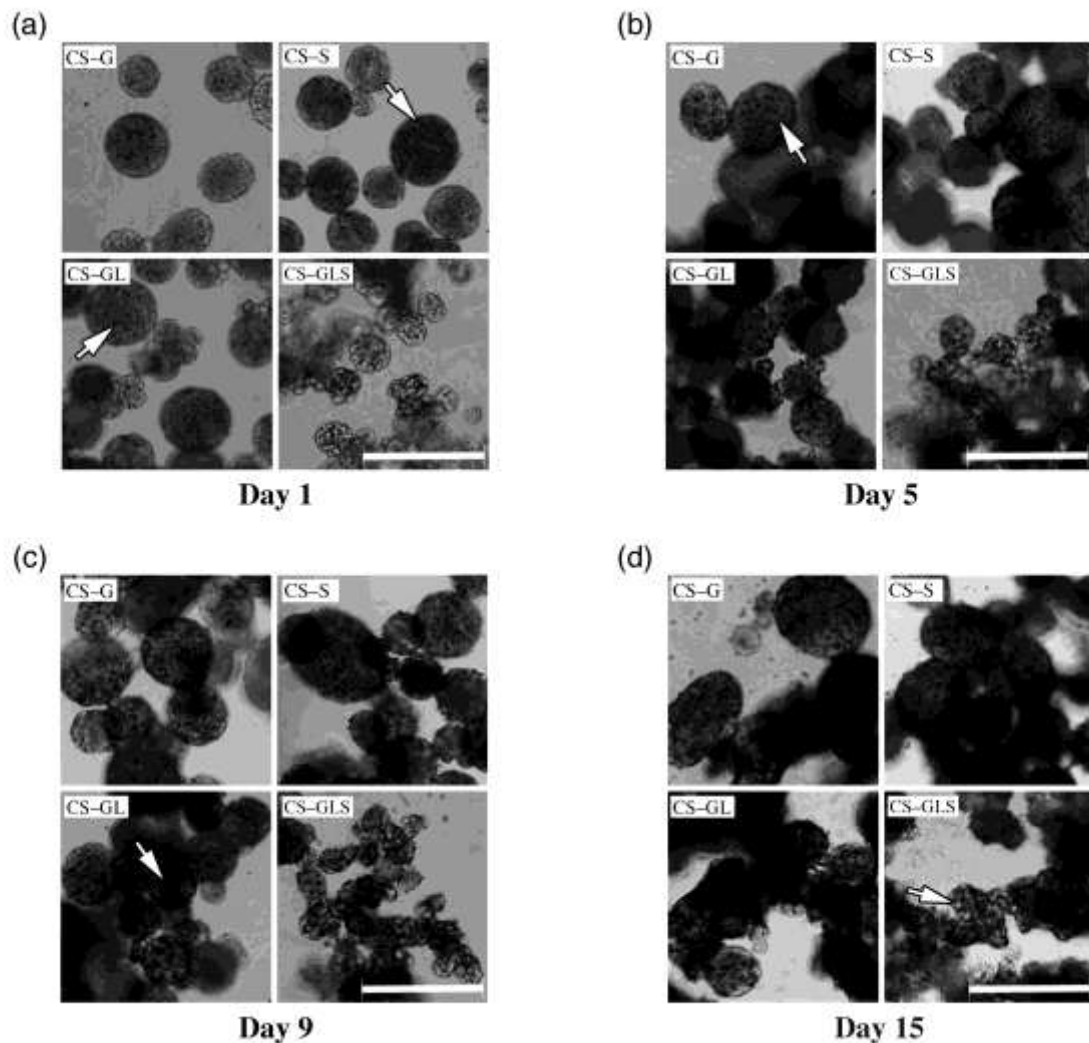


Figure 2. Viable chondrocytes (donor 2) were found adhered to the gelatine in all microcarrier groups. White arrows indicate examples of MTT-formazan reaction in the cytoplasm of viable cells on the microcarriers. Scale bar 250 μm .

3.3. Chondrocyte density

The total cell densities and corresponding regression lines, both normalized to 0.1 g dry weight gelatine mass, are presented for each unique data set in figure 3. Coefficients of determination (R^2), describing the percent variation of the data explained by the regression lines, ranged from 68.5% (figure 3l) to 93.3% (figure 3g) and averaged lowest for the CS-G microcarrier (74.6%) and highest for CS-GL (89.7%). For all microcarrier groups, the cell density increased from day 1 indicating

Microcarrier impact on chondrocyte expansion

ongoing proliferation of the adhered cells. No exponential growth phase was visible for the cell density curves. Rather, cell growth seems to have followed a linear pattern, indicating a limited cell growth. With the exception of some data series for the CS-GL (figure 3h) and CS-GLS (figure 3k) microcarriers, there were no signs of the cell density reaching a plateau. The data from all donors have been merged in figure 4a.

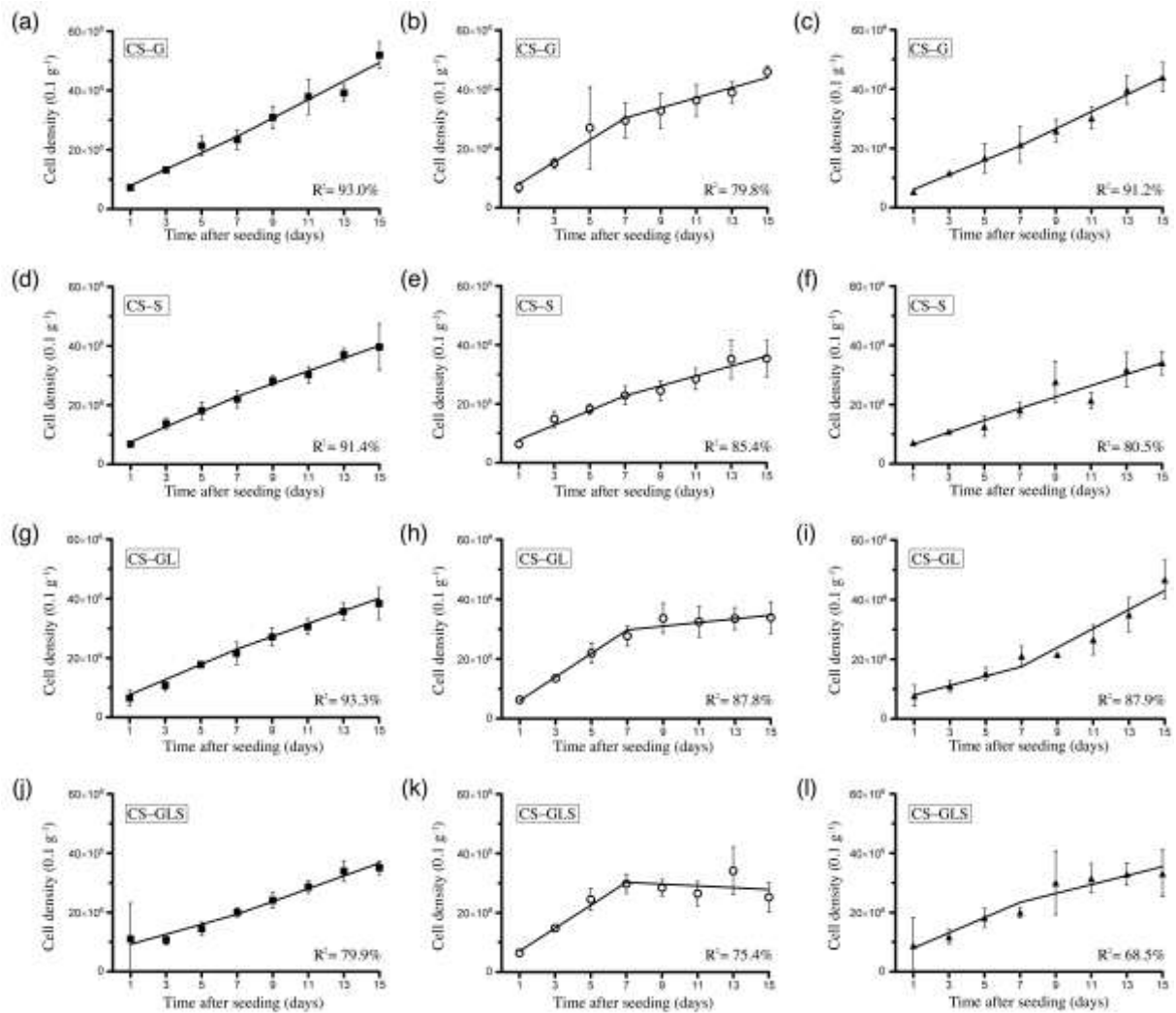


Figure 3. Cell density data for each microcarrier (mean±SD, n=5 for each data point) with corresponding regression lines and coefficients of determination, R². (Donor 1 – black square, donor 2 – hollow circle, donor 3 – black triangle).

A two-way ANOVA was performed for each time-point to investigate whether cell count means differed between microcarriers and/or donors. After 24 hours, we found no significant differences, indicating that initial cell adhesion to the matrices was independent on chondrocyte donor and did not differ between microcarriers. However a main effect of donor was found for the following three sampling times ($F(2,48) \geq 8.54$, $p \leq 0.018$), indicating diverse proliferation patterns depending on chondrocyte source once the cells had attached. From day 9 and forward, this simple donor effect was

Microcarrier impact on chondrocyte expansion

no longer present ($F(2,48) \leq 2.04$, $p \geq 0.05$). At the two last time-points, we found a main effect for microcarrier ($F(3,48) \geq 7.37$, $p \leq 0.019$), signifying that a significant difference in cell densities on the different scaffolds had emerged at the end of the culture period.

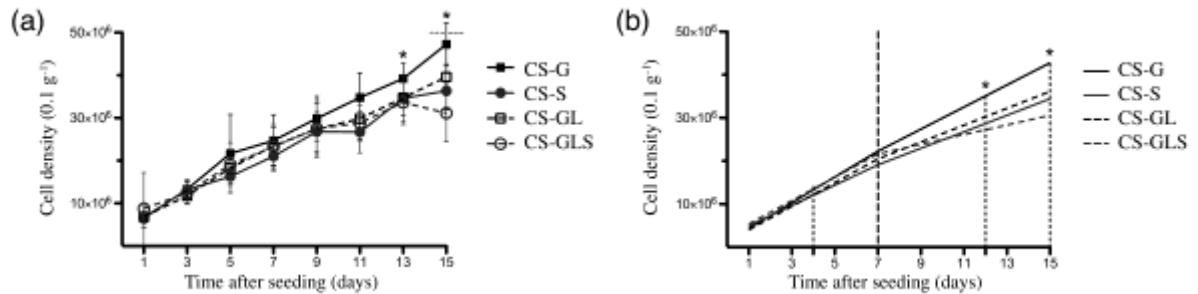


Figure 4. Cell density data for the expansion phase (a) using data from all donors (mean \pm SD, $n=3 \times 5$ for each data point). Corresponding piecewise linear regression curves (b) with a breaking point at day 7, indicated by a dashed line. ANOVA analysis for regression line levels was performed at day 4, day 12 and day 15, marked by dotted lines. Asterisks mark time points at which significant differences between microcarriers were found.

We further analyzed the differences between microcarriers using Tukey's pairwise comparison (table 3). At day 12, we found that the cell count for the CS-G microcarrier was significantly higher than all others, whereas there was no significant difference between the remaining groups. At the final time point, the chondrocyte density for the CS-G microcarrier was found to be significantly higher than the CS-GLS microcarrier.

Table 3. Tukey pairwise comparison of cell counts between microcarriers using CS-G as reference^a. Significant differences are marked with asterisks^b.

Microcarrier	Diff. of means ^c	SE of difference ^d	T-value	Adjusted p
<i>Day 13</i>				
CS-S	-46229	11745	-3.936	0.0293*
CS-GL	-45145	11745	-3.844	0.0324*
CS-GLS	-55853	11745	-4.756	0.0124*
<i>Day 15</i>				
CS-S	-109198	35141	-3.107	0.0757
CS-GL	-76523	35141	-2.178	0.2313
CS-GLS	-161041	35141	-4.583	0.0148*

^a For time points where significant differences between microcarriers were found.

^b No other significant differences between remaining microcarriers were found.

^c Difference of means compared to CS-G reference.

^d Standard error of difference.

Piecewise linear regression with a break point at day 7 was also conducted for each data set in order to facilitate comparison of chondrocyte growth on the microcarriers (figure 3 for individual regression lines and figure 4b for the merged data). A two-way ANOVA was conducted to investigate possible differences in the slope of the regression lines, corresponding to chondrocyte growth, before and after the breakpoint, as well as for how much the slope changed. We found decreases in regression

Microcarrier impact on chondrocyte expansion

line slopes for the merged data for all groups (figure 4b), however chondrocyte growth was not slowed for all donors and microcarriers (figure 3). The largest drop was seen for CS-GLS microcarrier, however the difference was not significant. In fact, the only main effect we found for regression line slopes was for donor, implicating that the chondrocyte source was the only factor that affected cell proliferation rate including by how much cell proliferation slowed during the second week ($F(2,6) \geq 5.65$, $p \leq 0.042$).

In addition, regression line levels, corresponding to chondrocyte density, were investigated in the middle of the first and second interval and at the final time point (figure 4b). In the middle of the first interval, corresponding to day 4, we found a main effect of donor ($F(2,6) = 10.88$, $p = 0.010$), however chondrocyte densities were not significantly different between microcarrier groups. In the middle of the second interval, corresponding to day 12 (figure 4b), and onward, this donor effect was no longer present. Instead, we found a main effect of microcarrier type ($F(3,6) = 11.55$, $p = 0.007$). This was also true for the following time point at day 15 ($F(3,6) = 8.96$, $p = 0.012$). These results indicate that chondrocyte density levels in the later stages of the culture period differed significantly between microcarrier groups. For these two time points, we also found main effects of the manufacturing procedures used to distinguish the microcarriers, i.e. emulsifier amount ($F(1,6) \geq 8.37$, $p \leq 0.028$) and cross-linking environment ($F(1,6) \geq 17.26$, $p \leq 0.006$), implying that chondrocyte levels differed significantly between microcarriers depending on their treatment during production. Tukey post-hoc tests for the regression line levels (table 4) at day 12 and day 15 revealed that the level for CS-G was significantly higher than for both the CS-S and CS-GLS microcarriers at this stage.

Table 4. Tukey pairwise comparison of regression line levels between microcarriers using CS-G as reference^a. Significant differences are marked with asterisks^b.

Microcarrier	Diff. of means ^c	SE of difference ^d	T-value	Adjusted p
<i>Day 12</i>				
CS-S	-70295	14953	-4.701	0.0131*
CS-GL	-50433	14953	-3.373	0.0554
CS-GLS	-81026	14953	-5.419	0.0066*
<i>Day 15</i>				
CS-S	-89755	24762	-3.625	0.0415*
CS-GL	-68545	24762	-2.768	0.1137
CS-GLS	-124276	24762	-5.019	0.0096*

^aFor time points where significant differences between microcarriers were found.

^bNo other significant differences between the remaining microcarriers were found.

^cDifference of means compared to CS-G reference.

^dStandard error of difference.

The differences in final cell yield between the groups followed the same pattern regardless of whether the cell count data or regression line levels were analyzed, with CS-G supporting the highest cell count, followed by CS-GL, CS-S and CS-GLS respectively. From the differences of means for the cell count data (table 3), we see that the difference between the CS-G and CS-GLS microcarriers at the final time point is -161041, translating into a difference of 16.1×10^6 cells per 0.1g microcarrier over a

Microcarrier impact on chondrocyte expansion

two-week period. By using the regression line level data (table 4), that difference is adjusted to 12.4×10^6 . The two-way ANOVA analysis of regression line levels indicated that manufacturing procedures affected the final cell yield. Using the differences of means from the regression line data (table 4), we can determine that the combined mean of microcarriers manufactured with high emulsifier amount (CS-GL and CS-GLS) is 51533 lower than the combined mean of their counterparts (CS-G and CS-S). This translates to approximately 5.15×10^6 fewer cells (normalized to 0.1g microcarrier as previously) over the two-week period. Using figures from the cell count data analysis (table 3), that difference is adjusted to 6.41×10^6 . Similarly, the combined mean of microcarriers cross-linked in water and acetone (CS-G and CS-GL) is 72743 higher compared to the mean of those cross-linked in water alone (CS-S and CS-GLS), translating into a difference of 7.27×10^6 cells over the culture period. Using figures from the cell count data analysis (table 3), the difference for cross-linking environment is adjusted to 9.69×10^6 .

3.4. Histology and immunohistochemistry

Following completed cell culture, the formaldehyde-fixed microcarriers were analyzed for extracellular matrix (ECM) formation. We found that modest to no ECM formation had occurred following the two week culture period as indicated by Alcian Blue and aggrecan staining results (data not shown). Large quantities of cells were found adhered to the microcarrier surfaces in a pattern consistent with the final MTT assay, whereas non-cellular areas were uncovered in the bulk of the sectioned scaffolds (data not shown). Results from the immunohistochemical analysis for intracellular chondrogenic markers revealed positive staining for SOX-9 (figure 5a) and S-100 (figure 5b). Positive staining correlated well with the presence of cell nuclei and non-specific cellular fluorescence was modest (figure 5c-d). There was no detectable fluorescence in negative controls.

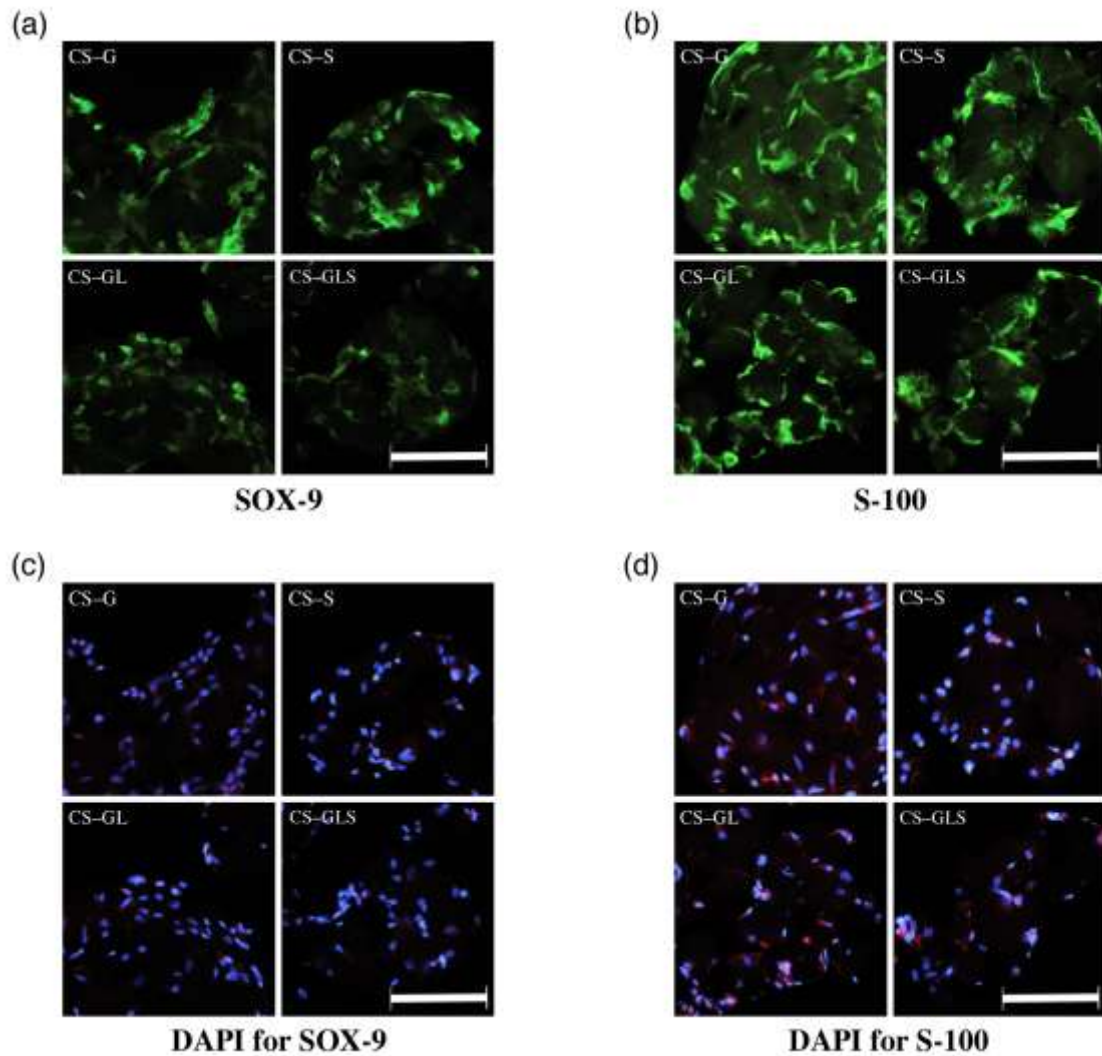


Figure 5. Immunohistochemical analysis of SOX-9 (a) and S-100 (b), with corresponding images retrieved in the same location with non-excitation filter combined with blue DAPI-stained cell nuclei (c, d), in formaldehyde-fixed microcarriers following 15 days of culture. All images are at the same magnification. Scale bars 50 μm.

4. Discussion

In the present study, cell expansion of human articular chondrocytes was evaluated on four types of macroporous gelatine microcarriers over a two-week culture period. The ability of this class of scaffold to support human chondrocyte growth is well known, yet to our knowledge this is the first time that a comparison between these four specific microcarriers has been conducted (Huss *et al.*, 2007; Malda *et al.*, 2003a; Pettersson *et al.*, 2009; Schrobback *et al.*, 2011).

Light and scanning electron microscopy was used to study possible differences in scaffold structure between the four groups. The CS-GL and CS-GLS microcarriers displayed larger pore diameters on the surface than their counterpart microcarriers, corresponding well with the reported difference (table 1, figure 1). Notably, the CS-GLS microcarrier distinguished itself with an irregular, less spherical shape. In all microcarrier groups, we found cases where regions on the beads displayed

Microcarrier impact on chondrocyte expansion

narrowed or closed pore openings. A similar pattern, with heterogeneous shapes of the external as well as internal pore structure, between individual microcarriers has been reported for the CS-G microcarrier previously (Bancel and Hu, 1996).

As expected, human articular chondrocytes adhered to and proliferated on all microcarriers, as illustrated by positive MTT-staining (figure 2) and an increase in cell density (figure 3) with time in all groups. The cell counts did not differ significantly between the microcarriers after 24 hours, indicating that initial adhesion to the microcarriers was quantitatively independent of microcarrier characteristics and chondrocyte origin. In comparison, Chinese hamster ovary cells demonstrated faster attachment to the CS-S microcarrier compared to the CS-G and CS-GL carriers (Kong *et al.*, 1999). At the first time point, we also noted several empty microcarriers (figure 2a). Bead-to-bead differences have been reported for this type of microcarrier, motivating the question whether preferential adhesion had occurred based on these differences (Bancel and Hu, 1996). However, chondrocytes populated all microcarriers with time (figure 2b–d), suggesting that the initial pattern was instead rather a result of random cell–microcarrier collisions in the spinner flasks.

The amount of time required to dissolve the microcarriers for cell counting increased with cell densities, as has been reported previously by others (Melero-Martin *et al.*, 2006). The ViaCount assay uses two fluorescent DNA-binding dyes with different permeability to distinguish between intact cells and cells with ruptured membranes (Ogasawara *et al.*, 2002; Phi-Wilson *et al.*, 2001). With this in mind, the prolonged exposure to trypsin in combination with the vigorous pipetting required to ensure a homogenous cell solution for cell counting procedures are potentially serious confounders. The viability data from the ViaCount assay was thus not used further. Instead, the total number of cells was used. The MTT assay can be used to ensure cell distribution and viability on the microcarriers, although it may not be possible to obtain accurate quantification of the percentage of viable cells. The lack of exponential growth phase indicated that cell growth was limited under the current conditions. Limited cell growth can be a sign of limited resources, such as inadequate oxygenation, nutrient depletion or insufficient surface availability. The formation of aggregates may have been a concern in this case. Aggregate formation has been reported in similar systems, with or without gelatine, and increases with cell densities (Melero-Martin *et al.*, 2006). Serum-free conditions can reduce the size and composition of chondrocyte aggregates in suspension culture, but does not inhibit aggregation altogether (Gigout *et al.*, 2005). Other suggested measures include a gradual increase of the agitation, but the accompanying fluid-induced shear is known to influence the metabolic expression of chondrocytes (Smith *et al.*, 1995). The linear increase in cell density may also be a sign of chondrocyte redifferentiation. Mature articular chondrocytes have a limited proliferation rate, but re-enter the cell cycle when expanded (Diaz-Romero *et al.*, 2005). Three-dimensional culture matrices, fluid flow-induced shear stress and hypoxia have all been shown to stimulate redifferentiation *in vitro* (Benya and Shaffer, 1982; Diaz-Romero *et al.*, 2005; Domm *et al.*, 2002; Malda *et al.*, 2003a; Murphy and Sambanis, 2001; Smith *et al.*, 1995; Malda *et al.*, 2004). This redifferentiation may also affect the

Microcarrier impact on chondrocyte expansion

proliferation rate of the chondrocytes, as the cells cease to divide in favour of ECM production (Lien *et al.*, 2008). However, we found little to no evidence of matrix production in the current study (figure 5).

The cell count data was analyzed using two approaches. First, cell count means were compared at each time point. Second, piecewise linear regression of each data set was performed. The latter approach enables comparisons of chondrocyte growth, corresponding to regression line slopes, and also takes results from neighbouring time points into consideration. Although the merged data for the microcarriers in figure 4 clearly displays a linear pattern, not all of the individual curves do (see for example donor 2 in figure 3c and donors 2-3 in figure 3d). To allow for donor differences, as well as the possibility that cell growth slows down during the later stage of the experiment (figure 4), piecewise linear regression with a break point at day 7 was used. In agreement, other studies have shown that chondrocyte proliferation decelerates or that the DNA content drops after approximately 7 days of culture (Melero-Martin *et al.*, 2006; Wu *et al.*, 2008; Grad *et al.*, 2003). Proliferation rates were indeed decreased for all microcarrier groups during the second half of the culture period, suggesting a similar pattern in our study. Only chondrocyte donor was found to influence proliferation patterns significantly, suggesting that microcarrier characteristics did not influence these events during this period. We also noted a main effect of cell donor on chondrocyte densities in the initial phase of the culture period, regardless of analysis approach. These results are in agreement with a recent study, investigating human chondrocyte expansion from three adult donors on CS-G microcarriers, revealing significant variations between donors (Schrobback *et al.*, 2011). In the current study, chondrocyte growth was significantly different between donors, yet the donor effect on cell density levels at day 12 and onward was not significant, indicating that the donor-to-donor variability influenced the manner in which the final cell density was reached, but not the end result.

Another shared result between the two analysis approaches was the emergence of microcarrier differences in the later stages of cell culture, yet there are discrepancies in the subsequent Tukey results. For instance, at day 15, the difference between the CS-G and CS-S cell count means is not significant whereas the difference in linear regression levels between these two groups is. For the preceding comparisons (day 12 and 13 respectively), the cell count data indicate that the CS-G mean is significantly higher than CS-GL (table 3), whereas the regression line levels of CS-G and CS-GL do not differ significantly (table 4). The results do however show a mutual pattern regarding the final cell yields, with the CS-G microcarrier supporting the highest chondrocyte number at the final time point, followed by CS-GL, CS-S and CS-GLS respectively. In this context, the irregular shape of the CS-GLS microcarrier is noteworthy. The differences of means (tables 3–4) indicate that higher chondrocyte densities can be achieved for microcarriers manufactured with a low emulsifier amount and subsequently cross-linked in water and acetone. The fact that no differences between the microcarriers were found during the initial culture phase implicates that microcarrier-based differences

Microcarrier impact on chondrocyte expansion

in chondrocyte proliferation may become apparent and/or detectable only during the later stages of the expansion phase.

As mentioned previously, the main differences between the microcarriers result from two varying manufacturing procedures. First, the amount of emulsifier used during initial emulsion steps can be used to control the average pore diameter of the interconnected pores (Nilsson, 2008). For the microcarriers tested in the current study, both microcarriers manufactured with high amounts of emulsifier (CS-GL and CS-GLS) demonstrated lower cell yields than their counterparts with smaller pore diameters (CS-G and CS-S), however not all differences were significant. Other authors have reported disparate results on the impact of pore diameter on cell proliferation. Porcine chondrocyte growth in chitosan sponges reached higher cell densities with increasing pore diameters, but there was no significant effect of pore diameter in rabbit chondrocyte proliferation on woven chitosan-hyaluronic acid scaffolds (Griffon *et al.*, 2006; Yamane *et al.*, 2007). For porous gelatine scaffolds, Lien *et al.* reported higher rat chondrocyte densities for scaffolds with pore diameters between 50–200 μm compared to scaffolds with pore diameters ranging between 250–500 μm , while glycosaminoglycan (GAG) production was higher in the scaffolds with larger pore diameters (Lien *et al.*, 2008). These diameters are however much larger than those investigated here. Interestingly, the pore diameters reported for the CultiSpher microcarriers lies in the range where the diameter of interconnections becomes critical for human osteoblast penetration in porous bioceramics (Lu *et al.*, 1999). In that study, the diameter also proved important for when formation of chondroid tissue or mineralized bone would occur. Importantly, other effects of surfactant concentrations on biomaterial characteristics have been reported, varying with respect to the biomaterial and manufacturing protocols (Dinarvand *et al.*, 2005; Jones and Hench, 2003; Yoon *et al.*, 2008). For gelatine microspheres, an increased surfactant concentration (Tween 85) led to a diminished particle size, a transition from a wrinkled to smooth surface characteristic as well as the introduction of craters (Esposito *et al.*, 1996). Notably, these spheres were manufactured at substantially higher temperatures. According to the ANOVA analysis of regression lines, the emulsifier concentration affected chondrocyte densities on the microcarriers in the later stages of our study. The current study does not give details whether this effect is based on a chondrocyte preference for a specific pore diameter or whether it is the result of altered surface characteristics.

The other difference during manufacturing concerns the environment in which the gelatine is cross-linked. In our study, analysis of the linear regression data shows that the CS-G microcarrier, manufactured in a mixture of acetone and water, yielded a significantly higher cell density than either S-type microcarrier, manufactured in water alone (table 4). This is in agreement with previous findings where rat chondrocytes were more abundant on collagen type II scaffolds prepared in acetic acid compared to scaffolds prepared in deionized water, regardless of whether the scaffolds were cross-linked with epoxy or carbodiimide (Tsai *et al.*, 2002). These findings may however be dependent on cell type, as the CS-S microcarrier supported higher cell densities of Chinese hamster ovary cells

Microcarrier impact on chondrocyte expansion

compared to CS-G and CS-GL carriers (Kong *et al.*, 1999). Gelatine has a high affinity for fibronectin and protein adsorption of fibronectin from the serum-containing cell culture medium enables fibronectin-mediated cell adhesion to the gelatine matrix in both cases. Tsai *et al* however reported that collagen scaffolds prepared in aqueous solutions had more hydrophilic surfaces than counterparts prepared in acetic acid (Tsai *et al.*, 2002). The different cross-linking environments may potentially have affected other scaffold properties as well, such as surface porosity, micropore size or microtopography, factors known to influence cell–surface interactions, including initial adhesion, cell morphology and proliferation (Boyan *et al.*, 1996; Costa Martinez *et al.*, 2008; Curtis and Wilkinson, 1997; Lee *et al.*, 1994). Naimark *et al* reported differences in mechanical and thermal behaviour of pericardial tissues following cross-linking by hexamethylene diisocyanate in different solvent environments (Naimark *et al.*, 1995). In addition, the methods used during gelatine cross-linking of electrospun scaffolds have been shown to affect fiber morphology (Sisson *et al.*, 2009). The authors speculated that the observed differences could depend on differential gelatine loss during the processes before cross-linking was completed. For the microcarriers used in this study, the same cross-linking agent was used, yet similar mechanisms may have lead to diverse gelatine loss and microcarrier characteristics during the cross-linking process. It has been reported that the CS-S microcarrier releases less gelatine into the media than the CS-G and CS-GL counterparts (Kong *et al.*, 1999). Although the CS-GLS microcarrier was not part of that study, it highlights a possible underestimation of the cellular density per gelatine mass. In the current study, we report that the G-type microcarriers have a higher cell density than the S-type equivalents per dry weight gelatine mass (see table 1 for microcarrier details). If these microcarriers have indeed lost more gelatine mass during the course of culture, the cell density per dry mass gelatine is likely an underestimation of the cell density per wet gelatine mass as well as of the difference in cell density between the two types of cross-linking environments reported here.

Following the culture period, remaining chondrocytes stained positive for both SOX-9 and S-100 after the 14-day expansion period, indicating that none of the investigated microcarriers caused a complete disappearance of the chondrocyte phenotype (Aigner *et al.*, 2003; Wehrli *et al.*, 2003; Wolff *et al.*, 1992; Zheng *et al.*, 2007). In accordance with the MTT assay results, large amounts of chondrocytes were found on the microcarrier surfaces, yet cellularity within the individual microcarriers was heterogeneous, consistent with previously reported patterns (Lim *et al.*, 1992). The incomplete population of the microcarriers may be attributed to previously discussed issues, such as aggregate formation, restricted access to the internal voids due to smaller openings at the surface (figure 1) or limited interconnectivity between the macropores (Borg *et al.*, 2009; Bancel and Hu, 1996). Sections stained for ECM molecules suggested that little or no ECM synthesis occurred during the two-week expansion phase, and we did not attempt to characterize this further. However, previous results have shown that human articular chondrocytes on gelatine microcarriers have produced an ECM rich in aggrecan, yet negative for collagen type II, after long-term culture with the currently used

Microcarrier impact on chondrocyte expansion

chondrocyte proliferation medium, highlighting the importance of cell culture conditions on chondrocyte metabolism (Blunk *et al.*, 2002; Jakob *et al.*, 2001; Malda *et al.*, 2003a; Pettersson *et al.*, 2009).

The current study focused on the effect of microcarrier selection on chondrocyte expansion using monolayer-expanded (P2–P3) human articular chondrocytes. It remains to be seen whether these results are generally applicable to all chondrocytes, including freshly isolated human cells (P0). The optimal result for chondrocyte expansion in tissue engineering applications may not be achieved by using one single technique, but by a combination of several techniques that momentarily guides the chondrocytes into a proliferative phase while protecting or enabling restoration of their full phenotypic capacity. Future studies are required to address the impact of microcarrier characteristics on the chondrogenic and metabolic expression of human articular chondrocytes in a three-dimensional setting.

In conclusion, all microcarriers investigated in this study supported chondrocyte adhesion and proliferation over a two-week period. Under the current conditions, the cell-yield obtained with the CS-G microcarrier was significantly higher than for both CS-S and CS-GLS. In addition, our results indicated that chondrocyte density levels were affected by the various manufacturing procedures, favouring microcarriers produced with a lower emulsifier content and cross-linked in a water and acetone solution.

Acknowledgements

The authors would like to thank Dr. Olle Eriksson for his help with the statistical analysis. This study was funded by the Swedish foundation for strategic research (Grant nr: A302:319) and the Materials in Medicine strategic research area (Linköping University and Landstinget i Östergötland).

References

- Aigner T, Gebhard P M, Schmid E, Bau B, Harley V and Poschl E 2003 SOX9 expression does not correlate with type II collagen expression in adult articular chondrocytes *Matrix Biol* **22** 363-72
- Bancel S and Hu W-S 1996 Topographical imaging of macroporous microcarriers using laser scanning confocal microscopy *J Ferment Bioeng* **81** 437-44
- Baschong W, Suetterlin R and Laeng R H 2001 Control of autofluorescence of archival formaldehyde-fixed, paraffin-embedded tissue in confocal laser scanning microscopy (CLSM) *J Histochem Cytochem* **49** 1565-72
- Benya P D and Shaffer J D 1982 Dedifferentiated chondrocytes reexpress the differentiated collagen phenotype when cultured in agarose gels *Cell* **30** 215-24
- Blunk T, Sieminski A L, Gooch K J, Courter D L, Hollander A P, Nahir A M, Langer R, Vunjak-Novakovic G and Freed L E 2002 Differential effects of growth factors on tissue-engineered cartilage *Tissue Eng* **8** 73-84
- Borg D J, Dawson R A, Leavesley D I, Huttmacher D W, Upton Z and Malda J 2009 Functional and phenotypic characterization of human keratinocytes expanded in microcarrier culture *J Biomed Mater Res A* **88** 184-94
- Boyan B D, Hummert T W, Dean D D and Schwartz Z 1996 Role of material surfaces in regulating bone and cartilage cell response *Biomaterials* **17** 137-46
- Chung H J, Kim I K, Kim T G and Park T G 2008 Highly open porous biodegradable microcarriers: in vitro cultivation of chondrocytes for injectable delivery *Tissue Eng Part A* **14** 607-15

Microcarrier impact on chondrocyte expansion

- Costa Martinez E, Rodriguez Hernandez J C, Machado M, Mano J F, Gomez Ribelles J L, Monleon Pradas M and Salmeron Sanchez M 2008 Human chondrocyte morphology, its dedifferentiation, and fibronectin conformation on different PLLA microtopographies *Tissue Eng Part A* **14** 1751-62
- Curtis A and Wilkinson C 1997 Topographical control of cells *Biomaterials* **18** 1573-83
- Diaz-Romero J, Gaillard J P, Grogan S P, Nestic D, Trub T and Mainil-Varlet P 2005 Immunophenotypic analysis of human articular chondrocytes: changes in surface markers associated with cell expansion in monolayer culture *J Cell Physiol* **202** 731-42
- Dinarvand R, Moghadam S H, Sheikhi A and Atyabi F 2005 Effect of surfactant HLB and different formulation variables on the properties of poly-D,L-lactide microspheres of naltrexone prepared by double emulsion technique *J Microencapsul* **22** 139-51
- Domm C, Schunke M, Christesen K and Kurz B 2002 Redifferentiation of dedifferentiated bovine articular chondrocytes in alginate culture under low oxygen tension *Osteoarthritis Cartilage* **10** 13-22
- Esposito E, Cortesi R and Nastruzzi C 1996 Gelatin microspheres: influence of preparation parameters and thermal treatment on chemico-physical and biopharmaceutical properties *Biomaterials* **17** 2009-20
- Eyrich D, Brandl F, Appel B, Wiese H, Maier G, Wenzel M, Staudenmaier R, Goepferich A and Blunk T 2007 Long-term stable fibrin gels for cartilage engineering *Biomaterials* **28** 55-65
- Fernandes A M, Fernandes T G, Diogo M M, da Silva C L, Henrique D and Cabral J M 2007 Mouse embryonic stem cell expansion in a microcarrier-based stirred culture system *J Biotechnol* **132** 227-36
- Fronzoza C, Sohrabi A and Hungerford D 1996 Human chondrocytes proliferate and produce matrix components in microcarrier suspension culture *Biomaterials* **17** 879-88
- Gigout A, Jolicœur M and Buschmann M D 2005 Low calcium levels in serum-free media maintain chondrocyte phenotype in monolayer culture and reduce chondrocyte aggregation in suspension culture *Osteoarthritis Cartilage* **13** 1012-24
- Grad S, Zhou L, Gogolewski S and Alini M 2003 Chondrocytes seeded onto poly (L/DL-lactide) 80%/20% porous scaffolds: a biochemical evaluation *J Biomed Mater Res A* **66** 571-9
- Griffon D J, Sedighi M R, Schaeffer D V, Eurell J A and Johnson A L 2006 Chitosan scaffolds: interconnective pore size and cartilage engineering *Acta Biomater* **2** 313-20
- Holtzer H, Abbott J, Lash J and Holtzer S 1960 The Loss of Phenotypic Traits by Differentiated Cells in Vitro, I. Dedifferentiation of Cartilage Cells *Proc Natl Acad Sci U S A* **46** 1533-42
- Huss F R, Junker J P, Johnson H and Kratz G 2007 Macroporous gelatine spheres as culture substrate, transplantation vehicle, and biodegradable scaffold for guided regeneration of soft tissues. In vivo study in nude mice *J Plast Reconstr Aesthet Surg* **60** 543-55
- Jakob M, Demartean O, Schafer D, Hintermann B, Dick W, Heberer M and Martin I 2001 Specific growth factors during the expansion and redifferentiation of adult human articular chondrocytes enhance chondrogenesis and cartilaginous tissue formation in vitro *J Cell Biochem* **81** 368-77
- Jones J R and Hench L L 2003 Effect of surfactant concentration and composition on the structure and properties of sol-gel-derived bioactive glass foam scaffolds for tissue engineering *J Mater Sci* **38** 3783-90
- Kong D, Chen M, Gentz R and Zhang J 1999 Cell growth and protein formation on various microcarriers *Cytotechnology* **29** 151-8
- Kuijpers A J, Engbers G H, Krijgsveld J, Zaat S A, Dankert J and Feijen J 2000 Cross-linking and characterisation of gelatin matrices for biomedical applications *J Biomater Sci Polym Ed* **11** 225-43
- Lee S J, Lee Y M, Han C W, Lee H B and Khang G 1994 Response of human chondrocytes on polymer surfaces with different micropore sizes for tissue-engineered cartilage *J Appl Polym Sci* **92** 2784-90
- Lien S M, Ko L Y and Huang T J 2008 Effect of pore size on ECM secretion and cell growth in gelatin scaffold for articular cartilage tissue engineering *Acta Biomater*
- Lim H S, Han B K, Kim J H, Peshwa M V and Hu W S 1992 Spatial distribution of mammalian cells grown on macroporous microcarriers with improved attachment kinetics *Biotechnol Prog* **8** 486-93
- Lippens E and Cornelissen M 2010 Slow cooling cryopreservation of cell-microcarrier constructs *Cells Tissues Organs* **192** 177-86
- Liu J Y, Hafner J, Dragieva G, Seifert B and Burg G 2004 Autologous cultured keratinocytes on porcine gelatin microbeads effectively heal chronic venous leg ulcers *Wound Repair Regen* **12** 148-56
- Lu J X, Flautre B, Anselme K, Hardouin P, Gallur A, Descamps M and Thierry B 1999 Role of interconnections in porous bioceramics on bone recolonization in vitro and in vivo *J Mater Sci Mater Med* **10** 111-20
- Malda J and Fronzoza C G 2006 Microcarriers in the engineering of cartilage and bone *Trends Biotechnol* **24** 299-304
- Malda J, Kreijveld E, Temenoff J S, van Blitterswijk C A and Riesle J 2003a Expansion of human nasal chondrocytes on macroporous microcarriers enhances redifferentiation *Biomaterials* **24** 5153-61
- Malda J, van Blitterswijk C A, Grojec M, Martens D E, Tramper J and Riesle J 2003b Expansion of bovine chondrocytes on microcarriers enhances redifferentiation *Tissue Eng* **9** 939-48

Microcarrier impact on chondrocyte expansion

- Malda J, van Blitterswijk C A, van Geffen M, Martens D E, Tramper J and Riesle J 2004 Low oxygen tension stimulates the redifferentiation of dedifferentiated adult human nasal chondrocytes *Osteoarthritis Cartilage* **12** 306-13
- Mauck R L, Wang C C, Oswald E S, Ateshian G A and Hung C T 2003 The role of cell seeding density and nutrient supply for articular cartilage tissue engineering with deformational loading *Osteoarthritis Cartilage* **11** 879-90
- Melero-Martin J M, Dowling M A, Smith M and Al-Rubeai M 2006 Expansion of chondroprogenitor cells on macroporous microcarriers as an alternative to conventional monolayer systems *Biomaterials* **27** 2970-9
- Murphy C L and Sambanis A 2001 Effect of oxygen tension and alginate encapsulation on restoration of the differentiated phenotype of passaged chondrocytes *Tissue Eng* **7** 791-803
- Naimark W A, Pereira C A, Tsang K and Lee J M 1995 HMDC crosslinking of bovine pericardial tissue: a potential role of the solvent environment in the design of bioprosthetic materials *J Mater Sci: Mater Med* **6** 235-41
- Nilsson K 1988 Microcarrier cell culture *Biotechnol Genet Eng Rev* **6** 403-39
- Nilsson K 2008 Porous gelatin material, gelatin structures, methods for preparation of the same and uses thereof. 7404971, United States <http://www.freepatentsonline.com/7404971.html>
- Ogasawara K, Yoshinaga S K and Lanier L L 2002 Inducible costimulator costimulates cytotoxic activity and IFN-gamma production in activated murine NK cells *J Immunol* **169** 3676-85
- Ohlson S, Branscomb J and Nilsson K 1994 Bead-to-bead transfer of Chinese hamster ovary cells using macroporous microcarriers *Cytotechnology* **14** 67-80
- Pettersson S, Wettero J, Tengvall P and Kratz G 2009 Human articular chondrocytes on macroporous gelatin microcarriers form structurally stable constructs with blood-derived biological glues in vitro *J Tissue Eng Regen Med* **3** 450-60
- Phi-Wilson J, Harvey J, Goix P and O'Neill R 2001 A technology for the rapid acquisition of cell number and viability *Am Biotechnol Lab* **19** 34-6
- Schroback K, Klein T J, Schuetz M, Upton Z, Leavesley D I and Malda J 2011 Adult human articular chondrocytes in a microcarrier-based culture system: expansion and redifferentiation *J Orthop Res* **29** 539-46
- Sisson K, Zhang C, Farach-Carson M C, Chase D B and Rabolt J F 2009 Evaluation of Cross-Linking Methods for Electrospun Gelatin on Cell Growth and Viability *Biomacromolecules*
- Smith R L, Donlon B S, Gupta M K, Mohtai M, Das P, Carter D R, Cooke J, Gibbons G, Hutchinson N and Schurman D J 1995 Effects of fluid-induced shear on articular chondrocyte morphology and metabolism in vitro *J Orthop Res* **13** 824-31
- Sommar P, Pettersson S, Ness C, Johnson H, Kratz G and Junker J P 2009 Engineering three-dimensional cartilage- and bone-like tissues using human dermal fibroblasts and macroporous gelatine microcarriers *J Plast Reconstr Aesthet Surg*
- Tsai C L, Hsu Sh S H and Cheng W L 2002 Effect of different solvents and crosslinkers on cytocompatibility of Type II collagen scaffolds for chondrocyte seeding *Artif Organs* **26** 18-26
- van Wezel A L 1967 Growth of cell-strains and primary cells on micro-carriers in homogeneous culture *Nature* **216** 64-5
- von der Mark K, Gauss V, von der Mark H and Muller P 1977 Relationship between cell shape and type of collagen synthesised as chondrocytes lose their cartilage phenotype in culture *Nature* **267** 531-2
- Wehrli B M, Huang W, De Crombrughe B, Ayala A G and Czerniak B 2003 Sox9, a master regulator of chondrogenesis, distinguishes mesenchymal chondrosarcoma from other small blue round cell tumors *Hum Pathol* **34** 263-9
- Werner A, Duvar S, Muthing J, Bunttemeyer H, Lunsdorf H, Strauss M and Lehmann J 2000 Cultivation of immortalized human hepatocytes HepZ on macroporous Cultispher G microcarriers *Biotechnol Bioeng* **68** 59-70
- Wolff D A, Stevenson S and Goldberg V M 1992 S-100 protein immunostaining identifies cells expressing a chondrocytic phenotype during articular cartilage repair *J Orthop Res* **10** 49-57
- Wu H, Wan Y, Cao X and Wu Q 2008 Proliferation of chondrocytes on porous poly(DL-lactide)/chitosan scaffolds *Acta Biomater* **4** 76-87
- Yamane S, Iwasaki N, Kasahara Y, Harada K, Majima T, Monde K, Nishimura S and Minami A 2007 Effect of pore size on in vitro cartilage formation using chitosan-based hyaluronic acid hybrid polymer fibers *J Biomed Mater Res A* **81** 586-93
- Yoon B H, Kim H E and Kim H W 2008 Bioactive microspheres produced from gelatin-siloxane hybrids for bone regeneration *J Mater Sci Mater Med* **19** 2287-92
- Zheng M H, Willers C, Kirilak L, Yates P, Xu J, Wood D and Shimmin A 2007 Matrix-induced autologous chondrocyte implantation (MACI): biological and histological assessment *Tissue Eng* **13** 737-46